Supramolecular Chemistry

Deutsche Ausgabe: DOI: 10.1002/ange.201706373
Internationale Ausgabe: DOI: 10.1002/anie.201706373

Supramolecular Nanotubules as a Catalytic Regulator for Palladium Cations: Applications in Selective Catalysis

Shanshan Wu[+], Yongguang Li[+], Siying Xie, Cong Ma, Joonwon Lim, Jiong Zhao, Dae Seok Kim, Minyong Yang, Doong Ki Yoon, Myongsoo Lee, Sang Ouk Kim, and Zhegang Huang**

Abstract: *Despite the recent development of highly efficient and stable metal catalysts, conferral of regulatory characteristics to the catalytic reaction in heterogeneous systems remains a challenge. Novel supramolecular nanotubules were prepared by alternative stacking from trimeric macrocycles, which was found to be able to coordinate with Pd cations. The Pd complexes exhibited a high catalytic performance for C–C coupling reaction. Notably, the tubular catalyst was observed to be controlled by supramolecular reversible assembly and showed superior heterogeneous catalytic activity, which was maintained for a number of cycles or reuse under an aerobic environment. Furthermore, the supramolecular catalyst showed unprecedented selectivity for the multifunctional coupling reaction and was able to serve as a new constructor of asymmetrical compounds.*

Developing highly efficient and stable metal catalysts has attracted great attention in chemistry and materials science because of both economic and environmental reasons.[1–4] In general, metal catalysts with small sizes are preferred owing to their high surface area for efficient catalysis. However, the reversible reaction of catalysis can result in serious aggregation of metal species, causing the gradual decrease of the catalytic activity.[5–7] For this reason, stabilizers such as surfactants,[8] polymers,[9–11] dendrimers,[12,13] silica,[14,15] and metal oxides[16–20] are actively investigated for preventing metal aggregation. Among them, sp^2-hybridized carbon materials are the most widespread supporting materials due to their low density, high surface area and ease of handling.[21–23] Introduction of a heteroatom such as nitrogen into conjugated carbon substrates would enhance electron capacity and thereby bind with metal atoms strongly.[24–26] Although ordered or disordered carbon-supported metal catalysts with remarkably enhanced activity have been successfully employed, they still have several deficiencies, including lack of long-term stability, low dispersibility, deactivation or constant leaching, as well as low recyclability, which limits their capacity and applications. Furthermore, the heterogeneous catalysts could not be controlled until the reaction is completed because of the difficult separation between the supporting materials and solvents during the reaction process, which is not suitable for multi- or selective catalysis.

Aromatic rod amphiphiles consisting of conjugated carbon and hydrophilic coil segments as the sp^2-hybrid carbon family can aggregate into porous structure to enhance the diffusion of bulky aryl substrates, and the transmission channels are well suitable as scaffolds for catalytic reaction in separated aromatic space.[27–32] Compared with the traditional supporting materials, the supramolecular substrates can be easily regulated by dynamic assembly through changing their environments because of their completely reversible formation.[33–36] For example, lateral attachment of hydrophilic oligoether segments into a linearly shaped aromatic rod leads the molecules to aggregate into toroidal nanostructures that are spontaneously connected with each other to form porous tubules in response to the aromatic guest.[37] The dynamic nature of the aggregates allows them to adapt the changes of pore surface to be more hydrophobic. As hinted from the adaptation by dynamic assembly, here we tried to align sandwich nanostructures with Pd ions as a catalytic core into hollow tubes to prepare the supramolecular porous catalyst. The supramolecular catalyst showed high efficiency for Suzuki–Miyaura (S-M) coupling reaction. Unlike conventional Pd catalysts, the catalyst could be used as the regulator for metal catalysis through dynamic assembly (Figure 1). Additionally, the catalyst recognized the size and type of starting materials and showed unprecedented selectivity for multifunctional S-M reaction, having potential to serve as a new concept for asymmetric catalysis.

The catalyst is derived from the self-assembly of a bent-shaped aromatic amphiphile containing a coordinative unit of pyridine at the inner position with a alkyl segment at both ends as hydrophobic segments, which was decorated by

[*] S. Wu,[+] Dr. Y. Li,[+] S. Xie, C. Ma, Prof. Dr. Z. Huang
PCFM and LIFM Lab, School of Chemistry, Sun Yat-sen University
Guangzhou 510275 (PR China)
E-mail: huangzhg3@mail.sysu.edu.cn
Dr. J. Lim, Prof. Dr. S. O. Kim
National Creative Research Initiative Center for Multi-Dimensional Directed Nanoscale Assembly, Department of Materials Science and Engineering, KAIST
Daejeon 34141 (Republic of Korea)
E-mail: sangouk@kaist.ac.kr
Prof. Dr. J. Zhao
Department of Applied Physics
The Hong Kong Polytechnic University
Hung Hom, Kowloon, Hong Kong (Hong Kong)
D. S. Kim, M. Yang, Prof. Dr. D. K. Yoon
Graduate School of Nanoscience and Technology and KINC
KAIST, Daejeon, 34141 (Republic of Korea)
Prof. Dr. M. Lee
State Key Laboratory for Supramolecular Structure and Materials
College of Chemistry, Jilin University
Changchun 130012 (PR China)
[+] These authors contributed equally to this work.

Supporting information for this article can be found under: https://doi.org/10.1002/anie.201706373.

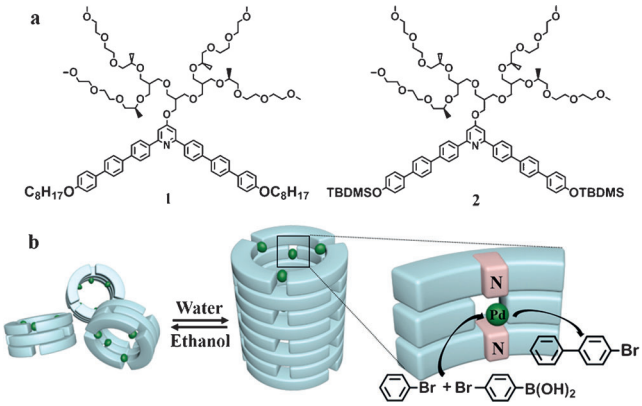

Figure 1. a) Molecular structures of 1 and 2; b) representation of the tubular regulator for the catalytic reaction based on reversible stacking of macrocycles.

hydrophilic oligoether dendron at its apex (Figure 1). To investigate the aggregation behavior of bent-shaped molecules, we have performed vapor pressure osmometry (VPO) experiments. The molecular weights of **1** based on an octyl-ended chain and **2** with a *tert*-butyldimethylsilyloxyl group were calculated to be 1713 and 1717 D, respectively. However, in the ethanol, the molecular weights of the primary aggregates were measured to be 5091 and 5212 D, respectively, which are three times as large as a single molecule (Supporting Information, Figure S2), suggesting that both noncovalent macrocycles from **1** and **2** consist of three single molecules.[36] Subsequently, the addition of water into the ethanol solution would drive the trimeric macrocycles to stack on top of each other to form hollow tubules. Figure 2a (Supporting Information, Figure S3) show micrographs obtained from a 0.02 wt% mixed solution ($EtOH/H_2O$ = 1:3) of **1** and **2** cast onto TEM grids. The TEM images of both samples show two parallel dark lines with a uniform distance of 4.0 nm. To further understand the aggregated nanosturctures, the scanning transmission electron microscope (STEM) experiment was implemented with a probe aberration corrector. STEM images show that the 1D objects were separated by dark and white segments, indicative of the formation of hollow tubules with an external diameter of 4.0 nm and a hollow interior with a diameter of 2.3 nm (Figure 2b; Supporting Information, Figure S3). When the membranes of **1** and **2** were transferred onto carbon-coated copper grids and then negatively stained with uranyl acetate, both the external diameters of the tubules were observed as 5.8 nm (Figure 2e; Supporting Information, Figure S3c). The external diameters of the tubules are identical to those of trimeric macrocycles, suggesting that the tubules originated from the macrocyles stacking. To gain insight into the packing arrangements of the rod segments within the 1D aromatic domains, we performed optical experiments. Upon addition of water into ethanol, both the absorption spectra of **1** and **2** displayed a blue-shifted absorption maximum and reduced fluorescence intensity compared with those in ethanol solution, indicating the H-type aggregates were formed from the aromatic segments (Supporting Information, Figure S4).[38] Circular dichroism (CD) spectra of the mixed solution of **1** showed a significant Cotton effect in the spectral range of the aromatic segments, indicating that the tubules adopt a one-handed helical structure (Figure 2f). To gain deeper insight into helical tubules, the atomic force microscopy (AFM) and two-dimensional X-ray diffraction (2D XRD) experiments were performed with thin membrane. Figure 3a shows two kinds of equidistant diffractions were observed at equator and meridian. The equidistant of 5.2 nm from equatorial diffractions corresponding to intercolumnar ordering, which is well-matched with the external diameter determined from TEM experiments. Meanwhile, several periodic reflections with equidistant of 2.8 nm were observed along the column axis. Taking into account the structure and dimensions of trimeric macrocycles, this diffraction pattern is attributable to a pitch of helical tubules. Indeed, the AFM image of **1** revealed the formation of a right-handed helical

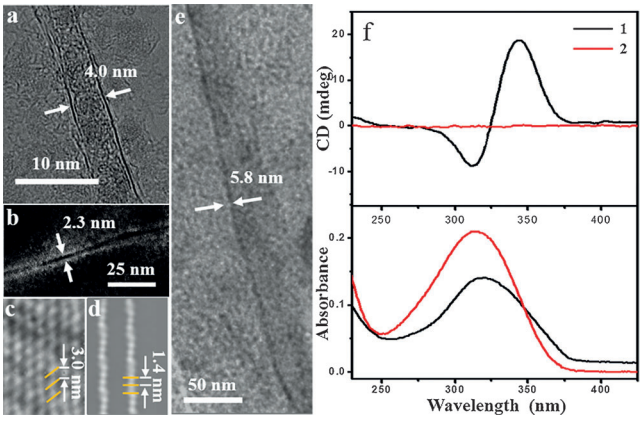

Figure 2. TEM, STEM, and AFM images and optical characterizations. a) TEM, b) STEM, and c) AFM images of 1 in ethanol–water mixture (1:3, v/v, 0.02 wt%). d) AFM image of 2 in ethanol–water mixture (1:3, v/v, 0.02 wt%). e) TEM image stained with uranyl acetate of 1 in ethanol–water mixture (1:3, v/v, 0.02 wt%). f) Absorption and CD spectra of 1 and 2 in ethanol–water mixture (1:3, v/v, 0.01 wt%).

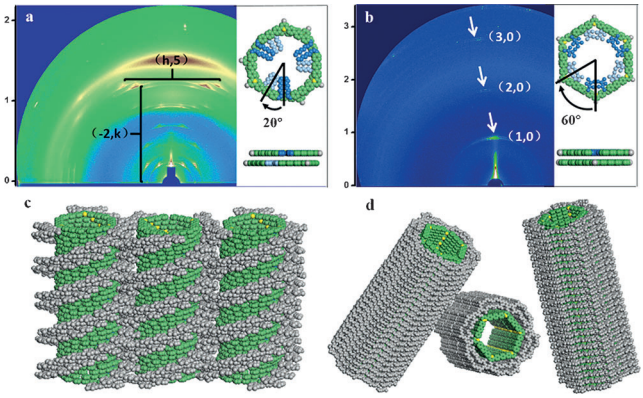

Figure 3. Stacked nanotubules from trimeric marcrocycles. 2D XRD patterns of a) 1 and b) 2 air-dried from mixed ethanol–water dispersions (1:3, v/v, 0.02 wt%). *y* axis: q space [$Å^{-1}$] (Inset: top and front views of oriented neighboring macrocycles) representation of the tubules based on c) helically ordering of 1 and d) alternative stacking of 2. Nitrogen atoms: yellow spheres, neighboring alkyl chains: blue and light blue, alkoxy chains: gray. Alkyl chains in (c) and (d) are omitted for clarity. For details see the Supporting Information, Figure S5.

structure with a pitch of 3.0 nm (Figure 2c), which is consistent with the CD and XRD results. These observations indicate that **1** self-assembles into the trimeric macrocycles, which, in turn, stack on top of each other with mutual rotation to form the right handed helical tubules.

We noticed that the tubular solution of **2** did not show CD signals within the area of aromatic absorption even though **2** contains chiral side groups (Figure 2f). For investigating the assembling geometries, we performed AFM measurements of the sample prepared by drop casting of the solution on a mica surface. The image clearly revealed that a periodically stacked 1D object with 6 nm diameter was formed (Figure 2d). The periodic structure was further analyzed by 2D XRD. The 2D image of **2** based on bulky alkyl segments displays sharp spots in same direction that correspond to equidistant *q*-spacings which indexed as 0.9 nm (Figure 3b). Given the interdistance from macrocycle stacking (0.45 nm), the space of 0.9 nm is approximately twice larger than that between neighboring cycles, suggesting the formation of non-chiral tubules with an alternatively cyclical stacking (Figure 3d). In contrast to **1**, there is large steric hindrance in the inside of trimeric macrocycles prepared from **2**. So the neighboring macrocycles stacked on each other without overlay of the bulky hydrophobic segments to reduce the contact between aromatic segments and solvents.

Owing to the periodical location of pyridine at the inner surface of the tubules, it is easy for the Pd cation to coordinate with pyridine, resulting in the formation of the supramolecular catalyst. The dispersion of Pd within self-assembled tubules displayed enhanced stability than dissolved state due to the sandwich structure (Supporting Information, Figure S6). In a mixed solution with $PdCl_2$, the Pd cation was successfully coordinated to the pyridine ligand with the observation of the red-shifted absorption band and significantly suppressed emission intensity (Supporting Information, Figure S7a,b). To take insight into the formation of supramolecular catalyst, X-ray photoelectron spectra (XPS) experiments were further performed. In the high-resolution spectra, a peak at 399.3 eV was observed and assigned to the pyridine nitrogen (1s).[39] However, the peak positively shifted to 400.1 eV in the supramolecular catalyst, confirming the existence of interaction between nitrogen and Pd (Supporting Information, Figure S7c).[40] The amount of Pd in tubules was determined by inductively coupled plasma atomic emission spectroscopy (ICP-AES), showing 92% of $PdCl_2$ formed the complexes on the inner pore of tubules. The molar ratio of nitrogen to palladium within the nanotubule was observed as 2.4:1 by semi-quantitative calculation from XPS experiments, which indicates Pd cation is coordinated by alternatively stacked pyridine (Figure 1).

Owing to the highly ordered porous structure and the significant stability for Pd cation at the porous walls, the Pd-coordinated tubule of **2** can be used as supramolecular catalysts with high active capacity for the S-M reaction with phenylboronic acid at ambient temperature. The tubular catalyst of **2** gave high catalytic conversions for all benzene halide (Supporting Information, Table S1, entries 1–3). With bulky substrates, however, the catalyst did not work as biphenyl substrates (Supporting Information, Table S1, entry 4). The results showed that biphenyl halide in this reaction was larger than the aperture of the tubules and the reaction could only occur for small benzene substrate. Notably, the tubular catalyst exhibited the switching behavior according to reversible self-assembly, and hence this supramolecular catalyst has served as the regulator for metal catalyst. As a result of poor diffusion of the reagents in molecularly dissolved state, the reaction could be halted immediately after the addition of ethanol to the reaction mixture leading to the deaggregation of the tubules, which induces the loss of catalytic activity. Thus, the conversion could also be monitored freely after the reaction was quenched. The conversion in real time is shown in the Supporting Information, Figure S8, demonstrating the catalytic reaction undergoes within 10 min with high conversion. Furthermore, the supramolecular catalyst exhibited high reusability under the reaction conditions with an aryl halide/molecule **2** molar ratio of 50:1. After completion of the reaction, the dissolved macrocycles were readily recovered by centrifugation. The catalyst was reformed after the addition of water and reused upon new reactants were added. After recycling procedures, we removed the catalyst and analyzed the reaction mixture by ICP-AES. No leaching Pd was detected during the disassembly and assembly processes, and the initial activity was completely maintained during five cycles of the reaction (Supporting Information, Figure S9). AFM and TEM studies clearly revealed that the reassembled tubules of **2** remains with same size and morphology even after exposure to the coupling reaction. Based on these results, we conclude that the tubular catalyst of **2** exhibits superior heterogeneous catalytic activity in terms of stability, recyclability, and reusability in C–C coupling reaction. In contrast to general Pd nanoparticles on solid supports, the catalyst additionally shows regulatory characteristics in the heterogeneous reaction by the supramolecular assembly and disassembly process.[5,10]

The special regulation with uniform porous surface motivated us to explore the selectivity of the S-M reaction using multifunctional substrate to develop new asymmetric coupling reactions. Thus, the reaction with bireactive sites was investigated with 4-bromophenylboronic acid and bromobenzene. It is known that the general Pd catalysts usually give aryl polymers or multiple products (Supporting Information, Table S1, entry 5). Remarkably, when the reaction was carried out by using tubular catalyst of **2**, the product of 4-bromobiphenyl was obtained reaching up to 90% within 30 min (Supporting Information, Table S1, entry 6). The probable reason for the high selectivity can be explained by spatial effect of tubular pores. As mentioned above, the aperture of tubular substrate is suitable for small benzene bromide, thus resulting in the enhanced activity for mono-coupling reaction.

In summary, we have demonstrated that stimuli-responsive supramolecular tubules through the self-assembly of trimeric macrocycles with alternative stacking can be used as catalytic regulator in heterogeneous system. The porous tubules from the self-assembly of N-substituted aromatic macrocycles provide a unique property to stabilize Pd cations on the inner surface against metal agglomeration, and provide

high catalytic activities during a number of recycles owing to its special sandwich construction for the stable formation of coordinated bond with Pd cation. Notably, the heterogeneous catalyst based on the self-assembled tubular substrate could be suspended and restarted conveniently through the supramolecular reversible assembly. Furthermore, the catalyst was endued with unprecedented selectivity within aryl polymerization owing to the spatial effect of tubular aperture. The special regulation with unprecedented selectivity for C–C reaction presented herein would provide a useful way to construct asymmetrical compounds with high catalytic activity.

Acknowledgements

This work was supported by Sun Yat-sen University, the NSFC (21302030), (21503284), Guangzhou Science and Technology Program (201707010248), the Key Laboratory of Functional Inorganic Material Chemistry (Heilongjiang University), Ministry of Education (2013kf05), and the Open Project of State Key Laboratory of Supramolecular Structure and Materials (sklssm2015011), the National Creative Research Initiative (CRI) Center for Multi-Dimensional Directed Nanoscale Assembly (2015R1A3A2033061). This work was also supported by the Hong Kong Polytechnic University Grant (No. G-YW1U, No. 1-ZE8C). Z.H. gratefully thanks the support from Harbin Institute of Technology.

Conflict of interest

The authors declare no conflict of interest.

Keywords: heterogeneous catalysis · nanostructures · self-assembly · supported catalysts · supramolecular chemistry

[1] L. L. Chng, N. Erathodiyil, J. Y. Ying, *Acc. Chem. Res.* **2013**, *46*, 1825 – 1837.
[2] W. A. Herrmann, *Angew. Chem. Int. Ed.* **2002**, *41*, 1290 – 1309; *Angew. Chem.* **2002**, *114*, 1342 – 1363.
[3] M. E. Davis, *Nature* **2002**, *417*, 813 – 821.
[4] D. Alberico, M. E. Scott, M. Lautens, *Chem. Rev.* **2007**, *107*, 174 – 238.
[5] C. T. Campbell, *Acc. Chem. Res.* **2013**, *46*, 1712 – 1719.
[6] M. Cargnello, V. V. T. Doan-Nguyen, T. R. Gordon, R. E. Diaz, E. A. Stach, R. J. Gorte, P. Fornasiero, C. B. Murray, *Science* **2013**, *341*, 771 – 773.
[7] N. P. Dasgupta, C. Liu, S. Andrews, F. B. Prinz, P. Yang, *J. Am. Chem. Soc.* **2013**, *135*, 12932 – 12935.
[8] M. T. Reetz, J. G. de Vries, *Chem. Commun.* **2004**, 1559 – 1563.
[9] G. Yun, Z. Hassan, J. Lee, J. Kim, N.-S. Lee, N. H. Kim, K. Baek, I. Hwang, C. G. Park, K. Kim, *Angew. Chem. Int. Ed.* **2014**, *53*, 6414 – 6418; *Angew. Chem.* **2014**, *126*, 6532 – 6536.
[10] R. Narayanan, M. A. El-Sayed, *J. Am. Chem. Soc.* **2003**, *125*, 8340 – 8347.
[11] R. Najman, J. K. Cho, A. F. Coffey, J. W. Davies, M. Bradley, *Chem. Commun.* **2007**, 5031 – 5033.
[12] K. R. Gopidas, J. K. Whitesell, M. A. Fox, *Nano Lett.* **2003**, *3*, 1757 – 1760.
[13] M. B. Lyudmila, B. S. Zinaida, *Chem. Rev.* **2011**, *111*, 5301 – 5344.
[14] C. M. Crudden, M. Sateesh, R. Lewis, *J. Am. Chem. Soc.* **2005**, *127*, 10045 – 10050.
[15] Y. Wan, H. Wang, Q. Zhao, M. Klingstedt, O. Terasaki, D. Zhao, *J. Am. Chem. Soc.* **2009**, *131*, 4541 – 4550.
[16] M. Zhao, K. Yuan, Y. Wang, G. Li, J. Guo, L. Gu, W. Hu, H. Zhao, Z. Tang, *Nature* **2016**, *539*, 76 – 80.
[17] H. Qi, P. Yu, Y. Wang, G. Han, H. Liu, Y. Yi, Y. Li, L. Mao, *J. Am. Chem. Soc.* **2015**, *137*, 5260 – 5263.
[18] Y. Lee, M. A. Garcia, N. A. F. Huls, S. Sun, *Angew. Chem. Int. Ed.* **2010**, *49*, 1271 – 1274; *Angew. Chem.* **2010**, *122*, 1293 – 1296.
[19] Z. Li, Z. Yuan, X. Li, Y. Zhao, S. He, *J. Am. Chem. Soc.* **2014**, *136*, 14307 – 14313.
[20] M. Choi, D.-H. Lee, K. Na, B.-W. Yu, R. Ryoo, *Angew. Chem. Int. Ed.* **2009**, *48*, 3673 – 3676; *Angew. Chem.* **2009**, *121*, 3727 – 3730.
[21] L. Qu, L. Dai, *J. Am. Chem. Soc.* **2005**, *127*, 10806 – 10807.
[22] S. H. Joo, S. J. Choi, I. Oh, J. Kwak, Z. Liu, O. Terasaki, R. Ryoo, *Nature* **2001**, *412*, 169 – 172.
[23] J. Lee, J. Kim, T. Hyeon, *Adv. Mater.* **2006**, *18*, 2073 – 2094.
[24] J. Tang, J. Liu, C. Li, Y. Li, O. M. Tade, S. Dai, Y. Yamauchi, *Angew. Chem. Int. Ed.* **2015**, *54*, 588 – 593; *Angew. Chem.* **2015**, *127*, 598 – 603.
[25] R. Arrigo, M. E. Schuster, Z. Xie, Y. Yi, G. Wowsnick, L. L. Sun, K. E. Hermann, M. Friedrich, P. Kast, M. Hävecker, A. Knop-Gericke, R. Schlögl, *ACS Catal.* **2015**, *5*, 2740 – 2753.
[26] L. He, F. Weniger, H. Neumann, M. Beller, *Angew. Chem. Int. Ed.* **2016**, *55*, 12582 – 12594; *Angew. Chem.* **2016**, *128*, 12770 – 12783.
[27] M. Lee, C. Jang, J. Ryu, *J. Am. Chem. Soc.* **2014**, *136*, 8082 – 8083.
[28] L. Y. Jin, J. Bae, J. Ryu, M. Lee, *Angew. Chem. Int. Ed.* **2006**, *45*, 650 – 653; *Angew. Chem.* **2006**, *118*, 666 – 669.
[29] A. C. Grimsdale, K. Müllen, *Angew. Chem. Int. Ed.* **2005**, *44*, 5592 – 5629; *Angew. Chem.* **2005**, *117*, 5732 – 5772.
[30] D. M. Vriezema, M. C. Aragones, J. A. A. W. Elemans, J. J. L. M. Cornelissen, A. E. Rowan, R. J. M. Nolte, *Chem. Rev.* **2005**, *105*, 1445 – 1489.
[31] J. Jiang, Y. Meng, L. Zhang, M. Liu, *J. Am. Chem. Soc.* **2016**, *138*, 15629 – 15635.
[32] J. Liu, T. Yang, D.-W. Wang, G. Q. Lu, D. Zhao, S. Z. Qiao, *Nat. Commun.* **2013**, *4*, 2798.
[33] V. Percec, A. E. Dulcey, V. S. K. Balagurusamy, Y. Miura, J. Smidrkal, M. Peterca, S. Nummelin, U. Edlund, S. D. Hudson, P. A. Heiney, H. Duan, S. N. Magonov, S. A. Vinogradov, *Nature* **2004**, *430*, 764 – 768.
[34] W. Jin, T. Fukushima, M. Niki, A. Kosaka, N. Ishii, T. Aida, *Proc. Natl. Acad. Sci. USA* **2005**, *102*, 10801 – 10806.
[35] L.-J. Chen, Y.-Y. Ren, N.-W. Wu, B. Sun, J.-Q. Ma, L. Zhang, H. Tan, M. Liu, X. Li, H.-B. Yang, *J. Am. Chem. Soc.* **2015**, *137*, 11725 – 11735.
[36] Z. Huang, S.-K. Kang, M. Banno, T. Yamaguchi, D. Lee, C. Seok, E. Yashima, M. Lee, *Science* **2012**, *337*, 1521 – 1526.
[37] E. Lee, J.-K. Kim, M. Lee, *J. Am. Chem. Soc.* **2009**, *131*, 18242 – 18243.
[38] M. Shirakawa, S. Kawano, N. Fujita, K. Sada, S. Shinkai, *J. Org. Chem.* **2003**, *68*, 5037 – 5044.
[39] A. E. Fernandes, S. Devillez, C. d'Haese, G. Deumer, V. Haufroid, B. Nysten, O. Riant, A. M. Jonas, *Langmuir* **2012**, *28*, 14822 – 14828.
[40] S. Gao, Y. Huang, M. Cao, T. Liu, R. Cao, *J. Mater. Chem.* **2011**, *21*, 16467 – 16472.

Manuscript received: June 23, 2017
Accepted manuscript online: July 14, 2017
Version of record online: & & & &, & & & &

Zuschriften

Supramolekulare Chemie

Die Ausrichtung von Sandwich-Nanostrukturen mithilfe aktiver Palladiumzentren ergibt einen supramolekularen Katalysator mit Nanoröhrenform (siehe Schema). Der reversible Auf- und Abbau des Katalysators stellt einen Steuermechanismus für die Metallkatalyse dar.